GAMMA RAY DOSE CALCULATIONS USING MONTE CARLO METHODS

by

S. PANDIMANI

NETP - 1906 - M - PAN - GAM

To

My parents

Srirangan

&

Rajalakshmisrirangan

CERTIFICATE

This is to certify that this work on "GAMMA RAY
DOSE CALCULATIONS USING MONTE CARLO METHODS% by
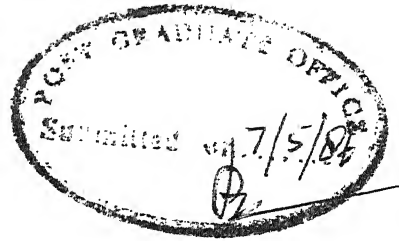Mr. S. PANDIMANI has been carried out under my supervision
and has not been submitted else where for the award of a
degree.

K. SRIRAM
Professor and Head
Nuclear Engineering and
Technology Programme
Indian Institute of Technology
Kanpur

ACKNOWLEDGEMENTS

ABSTRACT

Gamma Ray Dose calculations are done using Monte Carlo
Methods for a spherical shield geometry with a straight
cylinderical duct. All values obtained are for a disc source
placed at the center of the shield. All the three major
gamma ray interaction processess namely Photo electric effect,
Pair-Production and Compton scattering are included in the
simulation of Photon transport. Results are obtained for
dose points on the duct axis and also for points off the
duct axis. The latter shows that the scheme of particles
scoring used in the present work is not adequate and should
be modified.

CONTENTS

LIST OF FIGURES

LIST OF TABLES

CHAPTER-1

INTRODUCTION

Photon Transport studies are of great importance to Nuclear Scientists in shielding analysis and in other allied areas such as medicine. In practice, a few among these shielding problems can be handled by mathematical methods. The, then obtained analytical solutions or expressions are used to estimate the desired quantitites of interest such as dose, in a simple way.

Often Nuclear Engineers face problems which cannot be dealt by analytical methods because of irregular shapes in source and shield geometries. Shield geometry depends on the source geometry, the specific use of radio isotope etc.

Radiation streaming through ducts is also an important aspect in the design of shield. This problem was analysed by Tsuro et al (11) analytically. The shield geometry considered for their study is an infinite slab shield with finite thickness, having a cylinderical duct without any bend in it and the source is planar. Apart from research purposes, geometries with openings find extensive use in radiation therapy/non-destructive testing. One such geometry has been chosen for the present study and the geometry is finite in shape. Description and the problem of interest will be described in chap. 2.

Though analytical solutions are feasible to some extent for duct streaming problems, which are, in turn, derived with severe assumptions, one cannot have confidence over such solutions unless they are verified by some other methods and ultimately by experimental results. The same solutions become inapplicable when source and shield geometries are modified. For solving such radiation transport problems, probably Monte Carlo methods are suitable.

As is well known that all physical processes including the emission of radiation from sources and their subsequent transport through material are probabilistic in nature, i.e., one cannot predict with certainity what will happen for every individual particle in the process. Monte Carlo methods are used to simulate radiation transport through medium mathematically, through the use of various probability density functions. Density functions are the basic tools of Monte Carlo and are discussed in chap. 2.

For a photon radiation transport problem, two broad forms of Monte Carlo method are possible (12).

(i) Analogue Monte Carlo: In this method, the schematization followed closely resembles with the actual

physical process.

In this form, individual particle/histories are followed based on mathematical probabilities. Particles are created by sampling the governing density function of source which describes the behaviour of real particles. Each particle is followed until it survives in the medium of interest, shield for e.g.,and then a 'new' particle is started from the source. When large number of particles have been accounted, the accumulated data properly handled, will give the quantity of interest. So there is a strong analogy,in this approach, between physical and mathematical particles.

(ii) <u>Non-Analogue Monte Carlo</u>: Non-Analogue method is more sophisticated to solve a problem without any physical intution to real particles or processes. This method attempts to solve the transport equation straightaway.

Although non-analogue method is a versatile approach to solve transport problems, it is difficult to form exact transport equation for any arbitrary geometry. So more emphasis has been shown on analogue Monte Carlo method to investigate the chosen problem .

The main objective of this study is estimating the Gamma ray dose rates at some points of interest, for the chosen source and shield geometries. In order to facilitate the computations, following simplifications are made in developing a Monte Carlo code for the problem.

(i) Gamma rays interact with matter by more than ten distinctive processes. However, only three processes are significant to Nuclear Engineering problems and other processes can be neglected. These are 1) Compton scattering , 2) Photo-electric effect and 3) Pair-production.

(ii) All scattering interactions are assumed to be isotropic wherever it occurs in the system.

(iii) For a history, death can occur when the particle becomes absorbed, leaves the geometric region of interest or loses its significance owing to other factors (8).

In the Monte Carlo program, a system built-in function random number generator RAN(X) has been used throughout this work, which generates random numbers uniformly between 0 and 1.

CHAPTER-2

MONTE CARLO METHODS

This Chapter deals with the various steps involved in the simulation of photon transport. Though there may be more than one sampling technique applicable to a perticular step, sampling Compton energy, e.g., here, however, relevant sampling methods, say referred by earlier workers, are applied for each step of the simulation. Next section briefs the description of the problem of interest and the necessary steps involved in the simulation are discussed in the subsequent sections.

2.1 DESCRIPTION OF THE PROBLEM

Present work concentrates on a problem of calculating Gamma ray dose rates at some points of interest for a source and shield geometries as shown in Fig 2.1. Source geometry is a disc having uniform distribution over it. Shield geometry is a solid sphere with a cylinderical duct filled with some other material than shield material. Here, main object is to compute dose rates along the axis of cylinder and about the duct exit also. The latter can be interpreted by computing doses at different points on either sides along the perpendicular
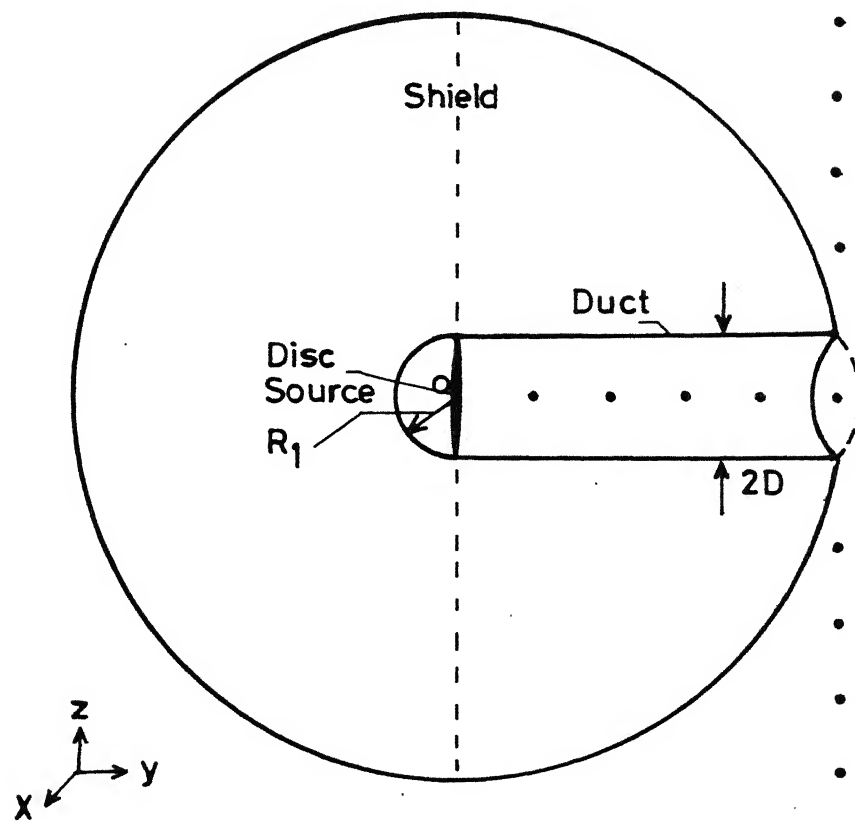
Fig. 2.1 Shield and Source Geometries

(a)

(b)
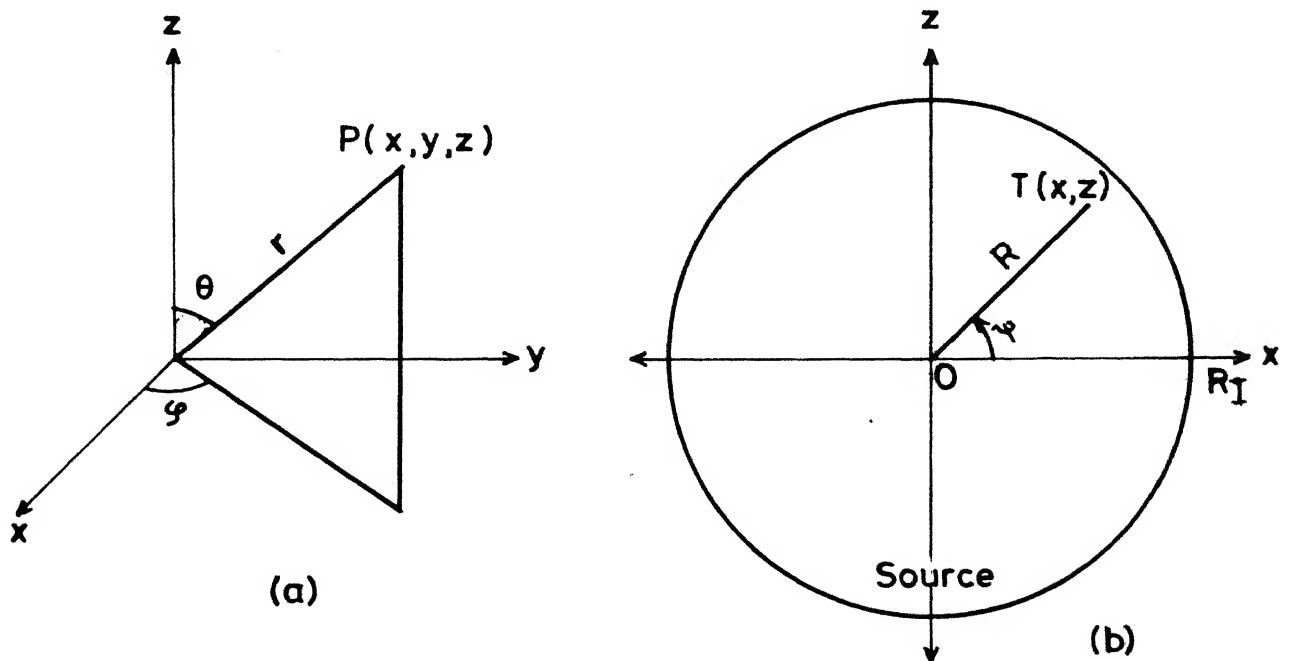
Fig. 2.2(a) Chosen Co-ordinate System-Spherical Polar Coordinate (b) Coordinate of a Source Point on the Disc Source.

to the axis of cylinder . Dose points of interest are shown
as dots in the same Fig. on the cylinder axis and on its
perpendicular also.

Spherical polar co-ordinate system is chosen to
represent these geometries in three dimension and the reference
axes X, Y and Z are shown in Fig. 2.2.a. Disc source lies
in the X-Z plane and cylinder axis coincides with the reference
Y axis. Shield radius is measured in m.f.p. units which is the
value at source energy for the shield material.

2.2 AN OVERVIEW OF ANALOG MONTE CARLO METHOD

As mentioned earlier, Gamma photons from a source
incident upon a shield and thereafter, its consequences
in the shield can, however, be realised mathematically by
using Analogue Monte Carlo Techniques. Particles coming from
a source have to be traced individually i.e.,from birth to
death or termination. Further divide the shield medium into
desired number of regions or zones according to the choice
of interest. The procedure to be followed is shown in
Figs. 2.3.a and 2.3.b.

This procedure may be repeated for a large number of
histories until the desired statistical acurracy is obtained.

START

READ input data
$\mu(E_i)$, $\mu_a(E_i)/\rho$, $i = 1,N$
IMAX: No. of histories
to be studied

INTERPOLATE $\mu(E)$s' and $\mu_a(E)/\rho$ s' for
any energy E_k between E_i and E_{i+1},
express Es' in Compton Units

$I = 1$

Study the history of
I^{th} particle. Call
subroutine HISPEE

$I = I + 1$

YES $I \leq IMAX$

NO

PRINT RESULTS
OF MONTE CARLO

STOP
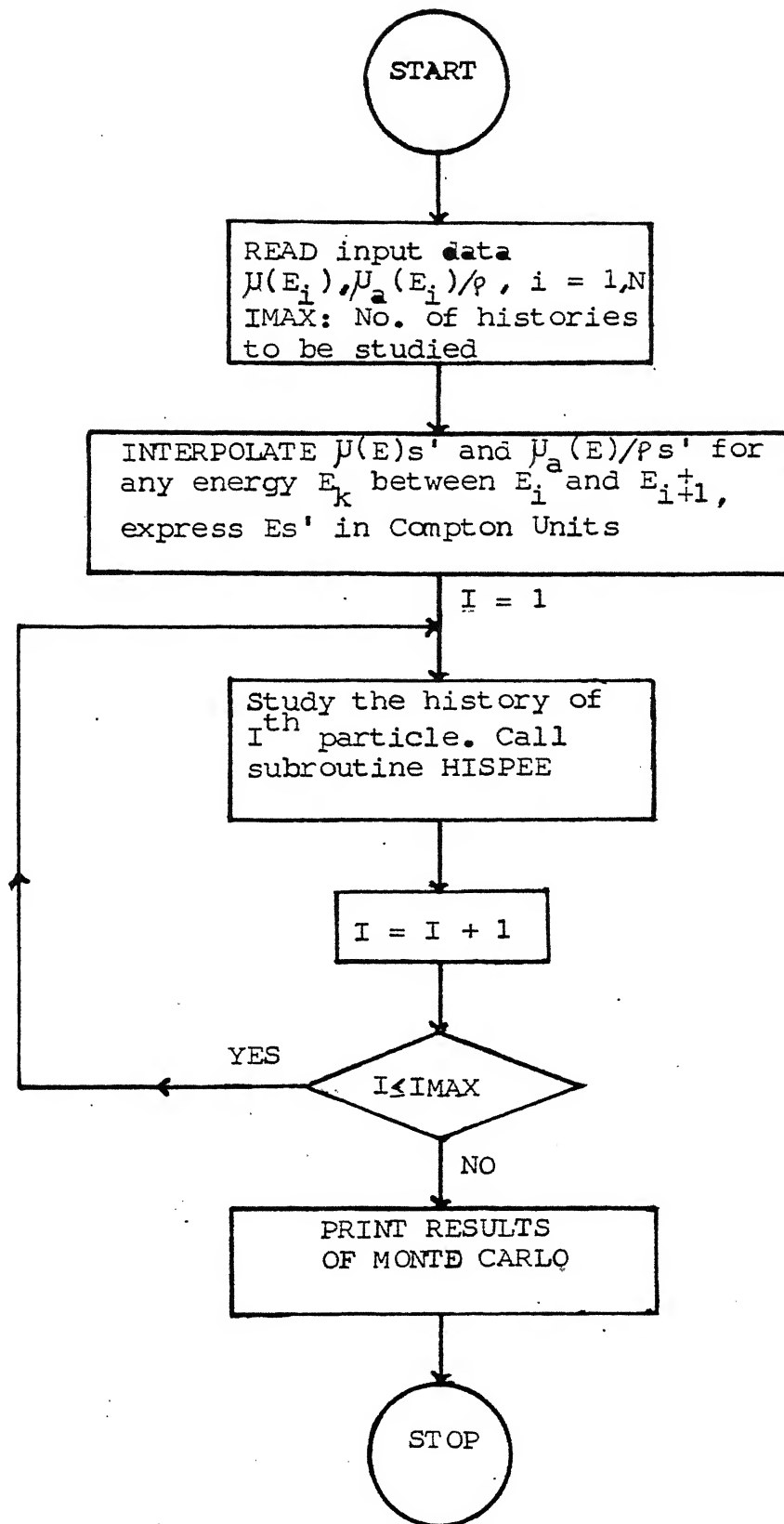
Fig. 2.3.a FLOW CHART FOR MONTE CARLO
MAIN PROGRAM
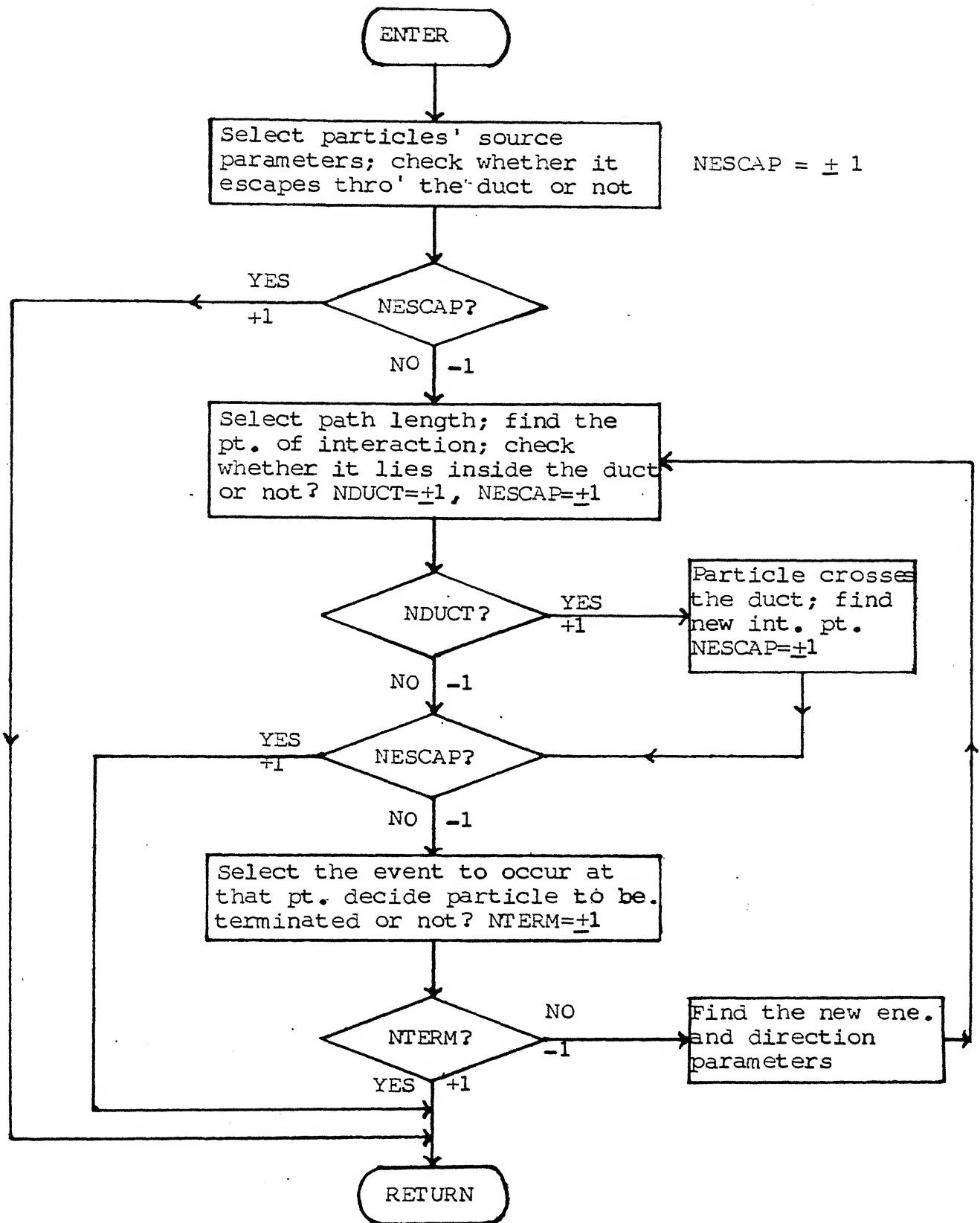
Fig. 2.3.b FLOW CHART FOR SUBROUTINE HISPEE

All steps given above are discussed in the next few sections in relevence to the chosen problem. A random process or event can be described mathematically by making use of the idea of probability density function (pdf) and cumulative distribution function (cdf) which are defined as follows:

(i) <u>Probability Density Function</u>: $p(x)$ describes the relative frequency of occurance of its random variable x (12). x can lie anywhere between $-\infty$ and $+\infty$. A pdf has the following properties:

$$1) \quad 0 \leq p(x) \qquad \text{for all } x$$

$$\text{and} \quad 2) \quad \int_{-\infty}^{+\infty} p(x) \, dx = 1$$

(ii) <u>Cumulative Distribution Function</u>: $C(X)$ gives the probability that a random variable x has a value less than or equal to a fixed value. It is defined by

$$C(X) = \int_{-\infty}^{X} p(x) \, dx = \text{prob}(x \leq X) \quad \ldots\ldots(2.1)$$

cdf has the following properties:

$$1) \quad \lim_{X \to +\infty} C(X) = 1$$

$$2)\quad \lim_{X \to -\infty} C(X) = 0$$

To sample a random value X from a given pdf, first select a value C(X) which is merely a number, essentially from numbers distributed uniformly between 0 and 1, then X can be obtained directly from equation(21) provided the corresponding pdf is a simple one, otherwise some other methods are to be followed to sample X.

2.3 SOURCE PARAMETERS

In order to initiate the problem, one has to startwith source particles i.e., photons and their parameters. Because, it is essential to know their spatial point of origin and direction of motion. A disc source is madeup of number of point sources. Since the choice of source parameters for a photon is not the same for different source geometries and for different source distribution like isotropic, cosine distribution etc., only uniformly distributed disc source and isotropic distribution for point source have been assumed throughout this work.

i) <u>Selection of Space Co-ordinates</u>: Consider the problem of choosing spatial co-ordinates for source particles. The

co-ordinates (x,0,z) of any point on the disc can be found interms of a selected random value R between 0 and radius of the disc, and ψ an angle randomly selected between $- \pi$ and $+ \pi$. R and ψ are shown in Fig. 2.2.b. The probability density function describing the distribution of sources distributed on a disc as a function of radius is $2 \pi R / \pi R_I^2$, where R_I is radius of the disc, and hence, the cumulative distribution function from equation (1) is (3)(8)

$$C(R) = \int_0^R \frac{2 \pi R dR}{\pi R_I^2} = R^2/R_I^2$$

using a random number 'r' between 0 and 1 instead of C(R) to select a random value of R directly from the above equation, it gives

$$r = R^2/R_I^2$$

It follows that

$$R = R_I \sqrt{r}$$

....(2.2)

From the fig. 2.2.b, it can be seen that for a given value of R, the source positions are equally distributed in azimuthal angle ψ between $- \pi$ and $+\pi$. Then selecting

for a random number 'r', it gives

$$r = \int_{-\pi}^{\psi} d\psi/2\pi = (\psi + \pi)/2\pi$$

or $\quad \psi = \pi(2r-1) \qquad\qquad\qquad \ldots\ldots(2.3)$

Now values of R and ψ are known. So point T(x,z) can be located on the disc from the equations $x = R \cos\psi$ and $z = R \sin\psi$.

ii) <u>Selection of Direction Parameters</u>: After assigning a spatial point of a source particle, or more precisely, after locating a point source on the disc, next consider the problem of assigning direction parameters to source particles. A disc source is symmetric w.r. to its axes i.e. it emits radiations equally on either sides. Further, a point source emits radiations into entire 4π steradians of solid angle. Here again, one can consider only a half of the sphere by taking the advantage of symmetry about a plane. So now the problem has reduced to a half sphere pointing towards +Y direction and hence, if a point is chosen on it, that point will give the necessary direction to the source particle. Ofcourse, that point may, however be expressed interms of direction cosines using a polar angle θ and an azimuthal angle ϕ .

Θ and $\emptyset$ are shown in Fig. 2.2.a. Selection of $\emptyset$ and Θ can be done in the following manner.

1) To select a polar angle ' Θ ' randomly anywhere between π and 0, the pdf interms of cosine of the angle 'k' — between -1 and +1 - is $\frac{1}{2}$ dk (3) and from this pdf, a random number r selected for the cdf gives directly,

$$r = \int_{-1}^{k} \frac{dk}{2} = \frac{k+1}{2}$$

or $k = 2r-1 = \cos \Theta$ .....(2.4)

2) To choose an azimuthal angle '$\emptyset$' between 0 and π, it is assumed that $\emptyset$ varies evenly in the interval 0 and π. So, for a random number 'r', choose $\emptyset$ to be equal to π r.

Finally, direction cosines for the source particle in spherical polar co-ordinates are obtained from the following equations using the values of Θ and $\emptyset$,

$$U_x = \mathrm{Sin}\Theta \ \mathrm{Cos}\emptyset$$

$$U_y = \mathrm{Sin}\Theta \ \mathrm{Sin}\emptyset \qquad \qquad .....(2.5)$$

$$U_z = \mathrm{Cos}\Theta.$$

U_x, U_y and U_z are the direction cosines along x, y and z directions respectively. A subroutine is written to compute space and direction co-ordinates of source particles using equations (2.2)-(2.5).

2.4 PATH LENGTH SELECTION

Thus, a set of source particle's parameters has been selected. Next, the path length from the source to the point of interaction has to be determined. The path length alongwith parameters of initial direction cosines defines the point at which interaction occurs. But, two mediums have to be considered for the geometry. Let duct be filled with air and the remaining part of the shield is made of lead. Only homogeneous medium has been considered wherever lead or air is present in the geometry. So before sampling the path length considering the duct, photons emanating from the source will fall into one of the following three cases listed below:

(i) A photon originating from the source may escape through the duct i.e., photon without even making any interaction with shield comesout of the duct freely passing through different mean free paths as shown in Fig. 2.4.a.
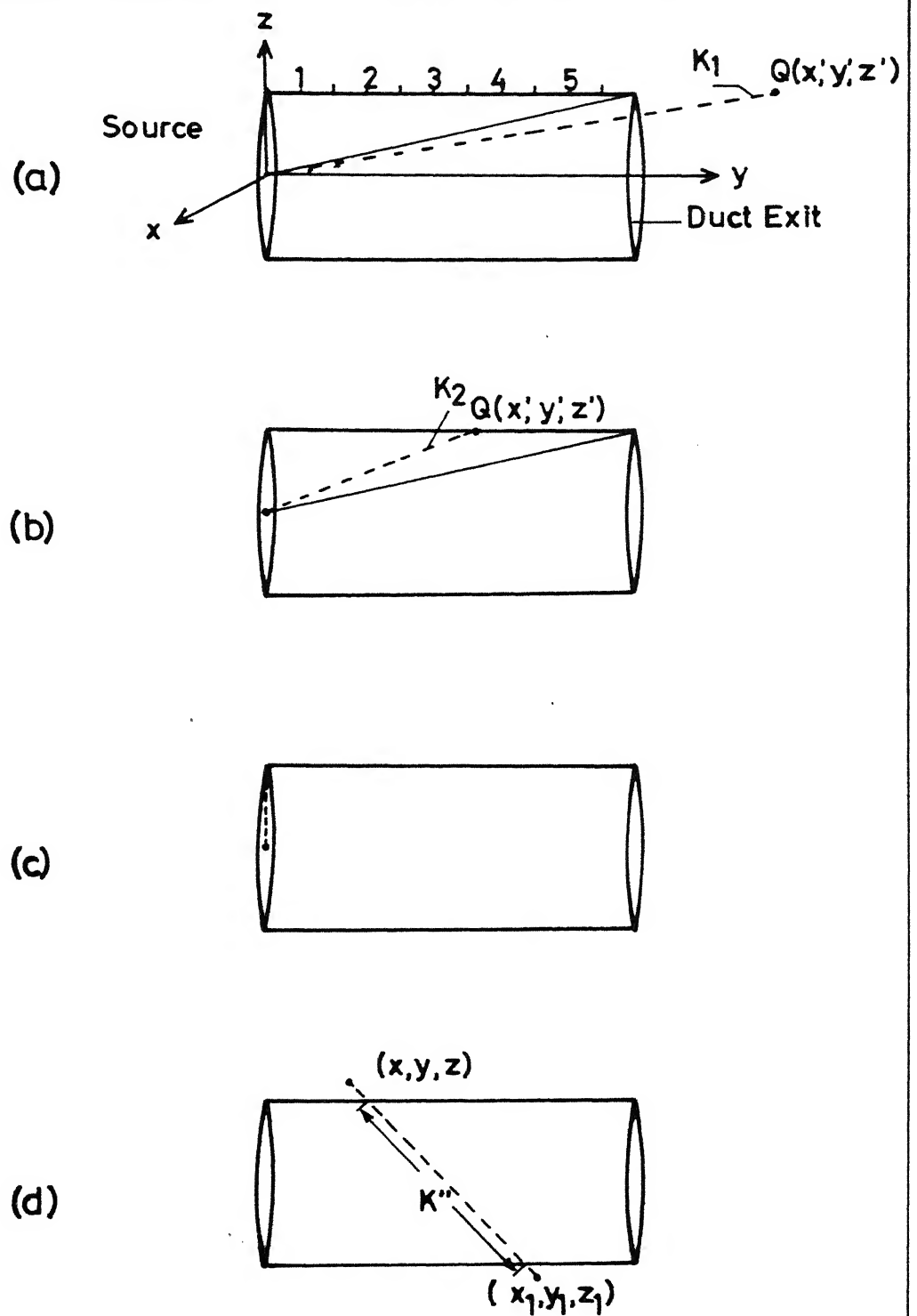
Fig. 2.4 Possible Particles Line of Flights.

This contributes a part to the uncollided or unscattered dose at the source energy. One m.f.p. in air at 1.25 MeV is approximately 13×10^3 cm whereas the whole spherical shield radius is approximately 9.0cm only and therefore, one can neglect the attenuation due to air throughout the particles line of flights.

Solving equation of a straight line and that of a cylinder will give 'k_1', where 'k_1' as shown in Fig. 2.4.a. The co-ordinates of that arbitrary point $Q(x',y',z')$ can be calculated using the following equations namely,

$$x' = x + U_x k_1$$

$$y' = y + U_y k_1 \qquad \qquad \ldots \ldots (2.6)$$

$$z' = z + U_z k_1$$

If $\sqrt{(x')^2 + (y')^2 + (z')^2}$ is greater than the maximum radius of the sphercial shield, then that photon will escape through the duct, otherwise it will not.

ii) The situation is shown in Fig. 2.4.b. Photon does traverse some distance 'k_2'-found in the same manner as 'k_1' - through the duct and the attenuation in air medium,

obviously, can be neglected, since $k_2 < k_1$. Hence particles co-ordinates have to be modified in order to keep track of the particle. Substituting k_2 in place of k_1 in equation (2.6) will yield the latest position of the particle with initial energy E_0, from where the particle will travel into shield by a distance equal to the selected value of the path length. However, direction parameters are retained for this purpose. In some other situations i.e., when R_1 is greater than duct radius, it may happen to travel some distance in air from its origin to the surface of inner cavity sphere. This is not shown in the figure.

(iii) In this case, photon does traverse no distance in air. Ofcourse, this will arise only when both source and shield are not separated by any distance from each other as shown in Fig. 2.4.c. and ofcourse, the chance of occurance of such case is very less unless the geometrical considerations are modified. So photon may be allowed to travel into shield directly just by sampling the path length. The selection procedure for the path length 'S' is as follows.

The probability of first collision between S and S + dS along the line of flight is given by (2)

$$p(S)\ dS = \mu\ e^{-\mu S}\ dS$$

where μ is the total linear attenuation coefficient of the shield material which gives the probability of collision per unit length. To sample S, cdf is given by

$$c(S) = \int_0^S \mu\ e^{-\mu S}\ dS$$

Select a value $C(S)$ using a random number r between 0 and 1 above equation becomes

$$r = \int_0^S e^{-\mu S}\ \mu dS = 1 - e^{-\mu S}$$

It follows that

$$S = -\frac{1}{\mu}\ \ln(1-r)$$

But $1 - r$ is distributed in the same manner as r. Therefore,

$$S = -\frac{1}{\mu}\ \ln r \qquad\qquad .....(2.7)$$

The selected path length 'S' together with direction cosines gives the point at which the photon interacts with the shield. Interaction may be any of the three events namely Compton scattering, Pair-Production and Photo electric effect. Sampling techniques applied for these three events will be discussed later.

2.5 NEW DIRECTION PARAMETERS

This section discuss the problem of finding new direction of a photon after it encountered a scattering or collision event. Consider a Compton scattering event occurs at some point in the shield. Once an elastic collision occured in a medium, its consequense results change in photons direction with loss in its energy. The situation is shown in Fig. 2.5.a. A method of sampling photon energy after collision will be discussed in later sections. . In this section, only particles new direction will be determined for a given scattering or deflection angle θ_0 and its local azimuthial angle as shown in Fig. 2.5.a and 2.5.b. θ_0 and $\emptyset_0$ are measured w.r. to particles initial direction. The new direction parameters will be very useful to maintain the track of a particle from its birth w.r. to a particular reference axes.

Having known old values of θ and $\emptyset$ and the values of θ_0 and $\emptyset_0$, the new direction parameters U_x', U_y' and U_z' are determined with the help of the following four equations where U_x', U_y' and U_z' are the modified direction cosines w.r. to different axes which are parallel to the
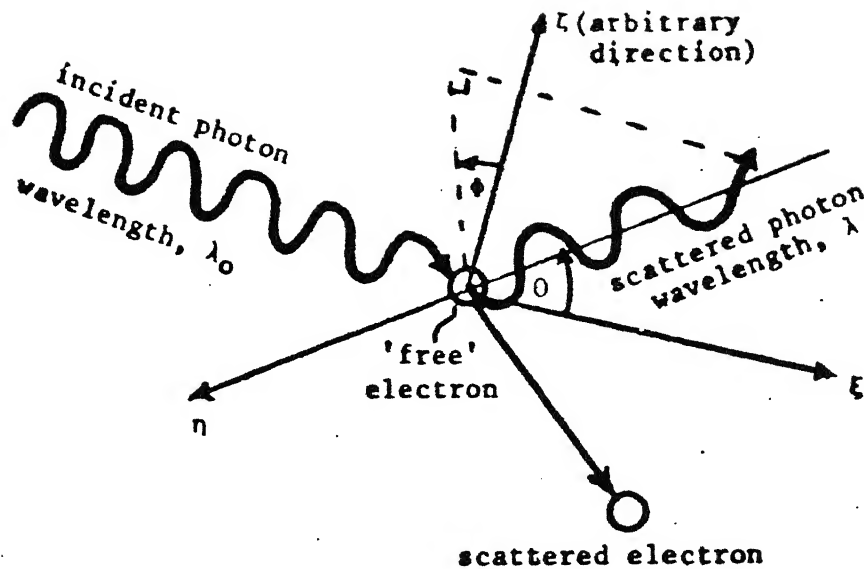
Fig. 2.5.a Compton scattering: an elastic collision between a photon and electron. The local orthogonal axes (ξ,η,ζ) are constructed such that ξ lies along the original direction of the photon's travel.
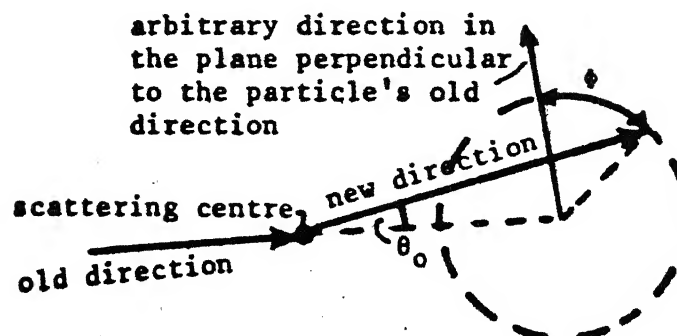
(Note:-) Particle's 'local' angles of scattering. θ_0 is the deflection angle, ϕ is the azimuthal angle. Usually the angle ϕ can be assumed to be randomly distributed in the range 0 to 2π.

Fig. 2.5.b Initial and Final Direction of Particle in Scattering

original reference axes X, Y and Z respectively.

$$\cos\Theta_n = \cos\Theta\cos\Theta + \sin\Theta\sin\Theta_o\cos\emptyset_o$$

$$\sin\Theta_n = \sqrt{1 - \cos\Theta_n \cos\Theta_n}$$

$$\cos\emptyset_n = \cos(\emptyset_o - \emptyset)\cos\emptyset - \sin(\emptyset_o - \emptyset)\sin\emptyset$$

and $$\sin\emptyset_n = \sin(\emptyset_o - \emptyset)\cos\emptyset - \cos(\emptyset_o - \emptyset)\sin\emptyset$$

Θ_n and $\emptyset_n$ are the modified polar and azimuthal angles respectively. The above four equations are taken from Wood and Ref.(6). According to Ref.(12), these equations are obtained by making use of trignometric relations. Once Θ_n and $\emptyset_n$ are known, U_x', U_y' and U_z' are readily found by substituting Θ_n, $\emptyset_n$ in place of Θ and $\emptyset$ in equation (2.5). Since the purpose of the above equations is to obtain the new direction parameters, much interest is not shown in the details of the derivation of them. The derivation may be seen in Ref. (12). In addition to the above method, few other methods are also proposed in Refs. (3) and (8).

2.6 ABOUT THE DUCT

With the knowledge of photons new direction parameters

and the new energy $E < E_o$ (E_o - initial energy), sample
a path length 'S' from equation (2.7) and calculate the next
interaction point using equations given below

$$x_1 = x' + U'_x S'$$

$$y_1 = y' + U'_y S'$$

and $\quad z_1 = z' + U'_z S'$ $\qquad \qquad \dots\dots(2.8)$

The next interaction point may face, apart from the type
of interaction, any one of the following three situations
given below:

(i) It may lie even outside the sphere or shield
or so to say, photon escapes from the shield with energy E.
Ofcourse, this can happen at any time independent of the number
of collisions. If a photon escapes from the shield then
ultimately its life history will be terminated.

(ii) It may lie within the shield. Here it is
essential to decide the type of event to be accounted,
depending upon that only, photon may either be allowed to
survive or not to survive.

(iii) Photon may encounter a situation as shown in Fig. 2.4d. i.e. photon crossing the duct. Here sampled path length 'S'' kept unaltered but it traverse an additional distance of 'k"' in air along that direction while crossing the duct. Whether photon crosses the duct or not can be found easily from the values of x_1, y_1 and z_1. So if a photon crosses the duct, then its actual point of interaction will be found just by substituting (S' + k") instead of S' in equation (2.8).

Further when a photon is allowed to cross the duct the point of interaction may or may not lie within the shield. In the former case, photon just crosses the duct and in the later case photon escapes through the duct; ultimately its termination.

2.7 SAMPLING TECHNIQUES

2.7.1 Compton Scattering: This effect is the scattering of a photon by a free electron which is at rest. In this interaction, photon loses some of its energy from its original value E_o to some other value E (E_o > E) and is deflected by an angle θ_o from its original direction of

motion (see Fig. 2.3.a). The relationship between E_O, E and Θ_O expressed interms of Compton wavelengths units namely $\bar{\lambda} = 0.511/\ \bar{E}$, where $\bar{E}$ is the photon energy in MeV, is

$$\lambda - \lambda_o = 1 - Cos\Theta_O$$

where λ_O and λ are the wavelengths before and af ter scattering respectively and ($\lambda - \lambda_O$) gives the increase in wavelengths which corresponds to the decrease in energy $(E_O - E)$.

In Monte Carlo calculations, it is necessary to know after a Compton scattering, the value of λ and Θ_O. Sampling from Klein-Nishina (K-N) scattering probability density function expressed interms of $X = \lambda / \lambda_O$ would suffice this requirement.

Though there are many techniques available to sample X from the K-N pdf, Wood and Blomquist (1) suggest that the sampling technique valid for any incident photon energy and, ofcourse, the most widely used also, is that of Khan (7). The details of K-N can be seen in Ref.(12) and the derivation of

START

SELECT RANDOM NUMBERS ξ_1, ξ_2, ξ_3

YES $\xi_1 \leq \dfrac{1 + 2/\lambda_n}{9 + 2/\lambda_n}$ NO

CALCULATE
$$R = 1 + \frac{2\xi_2}{\lambda_n}$$

CALCULATE
$$R = \frac{1 + 2/\lambda_n}{1 + 2\xi_2/\lambda_n}$$

NO
(Reject R) $\xi_3 \leq 4\left(\dfrac{1}{R} - \dfrac{1}{R^2}\right)$?

$\xi_3 \leq \dfrac{1}{2}\left[(\lambda_n - R\lambda_n + 1)^2 + \dfrac{1}{R}\right]$?   NO
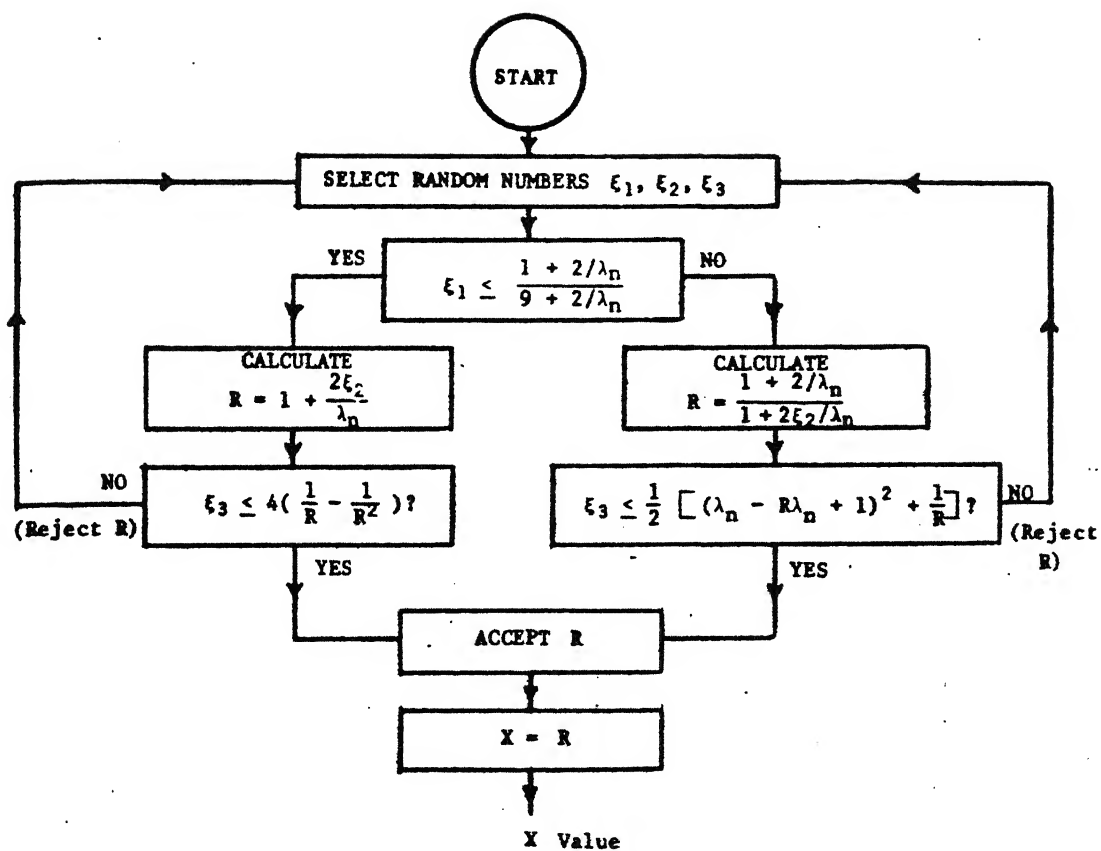(Reject R)

YES   YES

ACCEPT R

X = R

X Value

Fig. 2.6 Flow Chart for Kahn's procedure for sampling the K-N distribution to find the wavelength of a gamma photon after a Compton scattering.
λ_n is photon wavelength before scattering (assumed known), λ_{n+1} is photon wavelength after scattering and $X=R=\lambda_{n+1}/\lambda_n$.

Khan sampling technique may be seen in Ref.(1). The procedure
for sampling the K-N pdf to find the new wavelength ' λ '
is shown in Fig. 2.6.

Using the selected value of X shown above sampling
procedure, $\cos\theta_0$ can be obtained from the equation

$$\cos\theta_0 = 1.0 - \lambda_0 X + \lambda_0$$

Now the values of λ and θ_0 are known. Next, the azimuthal
angle $\emptyset_0$ may be selected in the following manner. As is
obvious, $\emptyset_0$ can have any values between 0 and 360^0, see
Fig. 2.5.b. This angle may be obtained by sampling at random,
assuming $\emptyset_0$ is distributed evenly in that range, as
$\emptyset_0 = 2\pi r$, where r is a random number between 0 and 1.

2.7.2 <u>Pair-Production</u>: This is an important reaction for
photon energies greater than 1.022 MeV. In this reaction,
the incident photon disappears in the field of charged particles
and an electron - positron pair appears with total energy equal
to that of photon. The energy (E - 1.022)MeV goes into
the kinetic energy of electron and positron pair. They
are attenuated in the medium. The electron eventually

original γ-photon
(E>1.022 MeV)

pair production interaction
occurs here: positron-electron
pair created

e⁻
electron eventually
absorbed in material

positron combines with
stray electron and is
annihilated

e⁻   e⁺

0.511 MeV
0.511 MeV
2-annihilation quanta created in
random, but opposite, directions
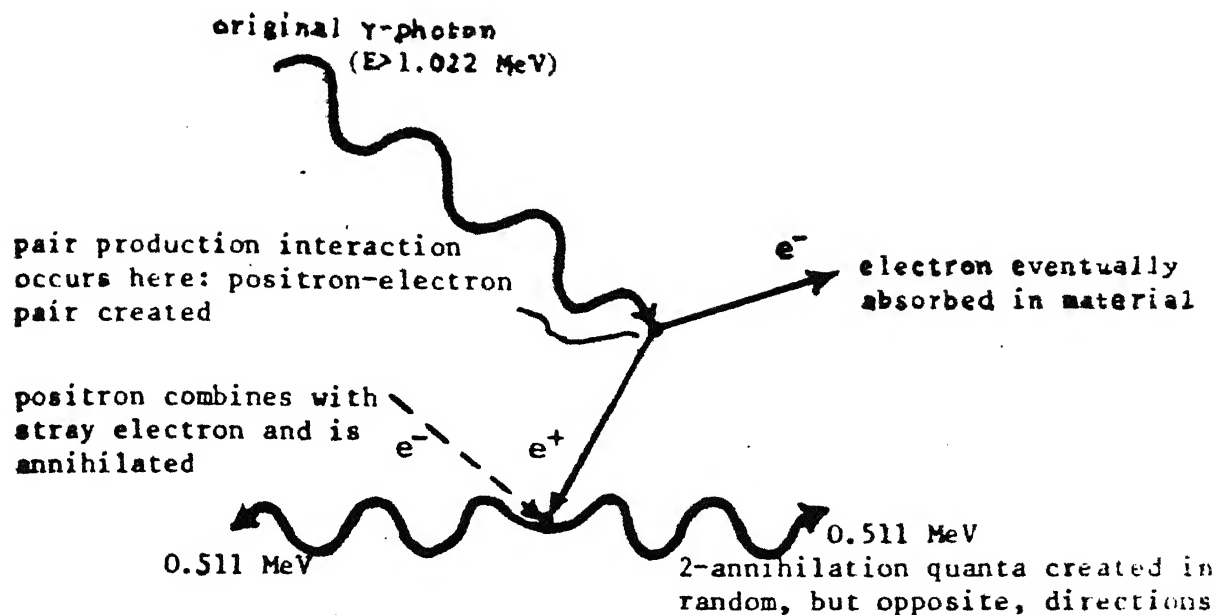
Fig. 2.7.a Scheme of the pair production process.

z'
γ
0.511 MeV
annihilation
gamma photon

θ_p

site of initial pair
production event
O'
y'

ϕ_p

0.511 MeV
γ annihilation
gamma photon
x'
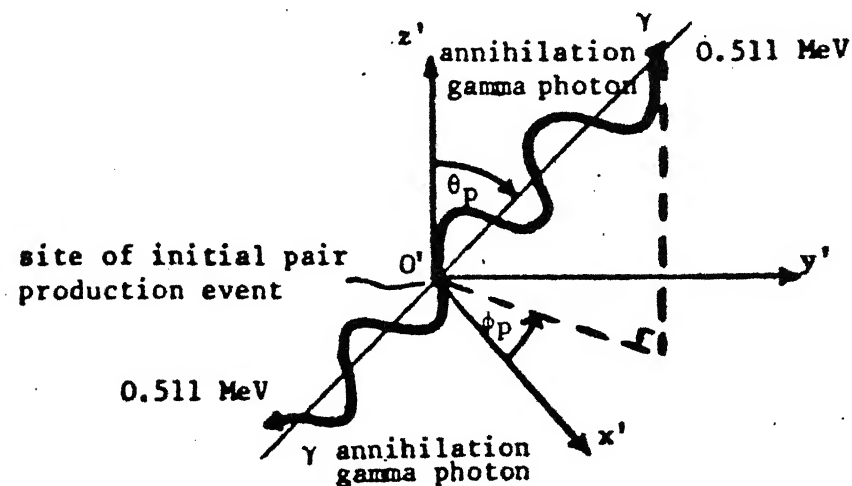
(Note:-) The 2-annihilation gamma photons are assumed to
emerge isotropically. That is, with respect to the ortho-
gonal axes (x', y', z'), the azimuthal angle ϕ_p is uniform-
ly distributed in the range 0 to 2π, and the cosine of θ_p
is uniformly distributed in the range -1 to 1.

Fig. 2.7.b Direction of Annihilation Gammas After
Pair-Production

absorbed while the positron combines with an electron in the
attenuating material and in this process two Gamma quanta
of 0.511 MeV (rest mass of electron) are released.

In Monte Carlo calculations, for accounting a
Pair-Production event,two assumptions are made. Firstly,
annihilation Gammas are released at the position at which
the Pair-Production occurs. Secondly, the two Gammas are
released at random in mutually opposite directions. They
are shown in Fig. 2.7.a.

Now, the initial direction of annihilation Gammas
has to be sampled. The sampling is done in the following manner.
Further, it is assumed that the angular distribution of
Gammas to be isotropic. That is, the cosine of θ_p, the polar
angle, is uniformly distributed in the range -1 to +1 and
the azimuthal angle $\emptyset_p$ is uniformly distributed in the range
between 0 and 2π. θ_p and $\emptyset_p$ are measured w.r. to parent
photon's direction and they are shown in Fig. 2.7.b.

According to Ref. (12), to reduce C.P.U. time,only
one annihilation Gamma from the pair can be followed; as

compensation, its weight must be multiplied by two. Concept of weight will be seen in Chap. 3. The error resulting from the above approximation is likely to be very small because of the random orientation with which annihilation quanta are released. Finally, the value of θ_p and $\emptyset_p$ are selected from the equations.

$$Cos\theta_p = 2r_1 - 1.0$$

and $$\emptyset_p = 2\pi r_2$$

where r_1 and r_2 are random numbers. Using these values the new direction parameters w.r. to the reference axes can be computed using the equation given in section 2.5.

2.7.3 Photo Electric Effect: It is an absorptive event and in this process, the incident photon is absorbed and depending upon its energy, an inner orbital electron (i.e. from k shell) is ejected. The vacancy created is filled by a transition of one of the outer shell electrons accompanying either a fluorescent emission or an Augar electron. This effect is very important for low energy photons in materials with high atomic numbers (Z). In this Monte Carlo calculations for Photo electric effect it is assumed that all transitions
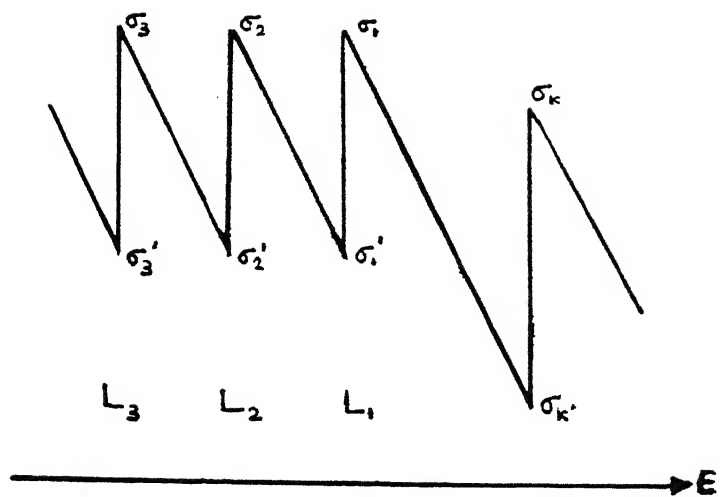
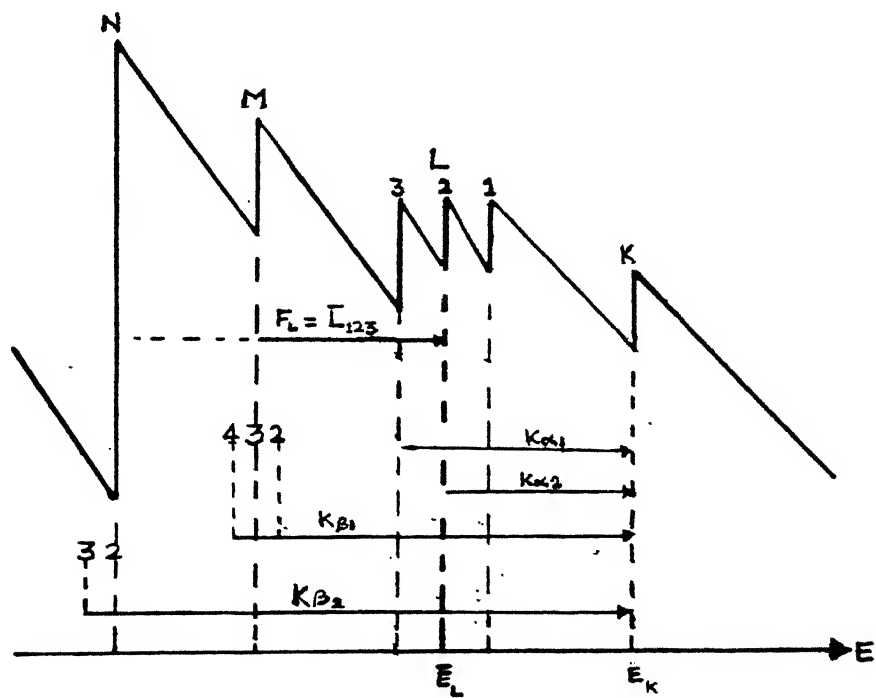Fig. 2.8.a K and L Edge Structures

Fig. 2.8.b Fluorescent "Lines"

are accompanied by the emission of fluorescent lines only. Thus, Augar electrons are completely neglected throughout this work.

The energies corresponding to K and L shells are called edge energies because the Photo electric cross section $\mathcal{G}_{pee}$(E) elsewhere decreasing continuously shows a sharp discontinuity (edge) at each of them (2). The behaviour at the K and L edges are shown in Fig. 2.8.a.

The energies E_K and E_L compared with the incident photon energy serve to determine the probability of K or L shell ejections. So when a photon of energy $E \gtrsim E_K$ is absorbed there is a likely chance of K-shell electron ejection with kinetic energy $(E - E_K)$. Further the vacancy created is filled by an electron from any one of the outer shells (L, M or N) making a transition accompanying a fluorescent emission. The possible K and L fluorescent emission or lines. K_{α_1}, K_{α_2}, K_{β_1}, K_{β_2} and F_L are shown in Fig. 2.8.b and their energies are given in Table 2.1. For elements with $Z > 31$, L - fluorescent emission is also possible.

If the incident energy E is greater than E_K, then

either K or L shell ejection is possible. Ofcourse outer shell ejection is **also** allowed. Now, one has to decide which ejection is to be considered. So some three numbers $\emptyset_K$, $\emptyset_L$ and $\emptyset_O$, which will determine the relative probabilities of K, L and outer shell ejections for $E \geq E_K$ and $\emptyset_L$, $\emptyset_O$ also define the chances of L or outer shell ejections, for $E_L \leq E < E_K$, are required.

The values of $\emptyset_O$, $\emptyset_L$ and $\emptyset_K$ are taken from Ref.[5] and are shown in Table 2.1. These values are computed using the Photo electric cross sections at various edges. Further, the yield Y_i for a shell i is the total probability of emission accompanying electron transition from all outer shells to a vacancy in shell i. The individual yields for K — lines and L — lines are shown in the same table. A random number lying between $\emptyset_{i-1}$ and $\emptyset_i$ implies i^{th} shell electron ejection and similarly a random number between $Y_{i-1} / \emptyset_{i-1}$ and $Y_i / \emptyset_i$ implies i^{th} fluorescent emission. Here also, the particle's statistical weight is modified and this concept will be discussed in Chap. 3. Next, the photon with new fluorescent energy has to be followed. This, as done before in case of Pair-Production, those two angles are sampled in

34

Table 2.1 Final values of $\emptyset_i$, Y_i and F_i

i	Shell	Edge Energies in MeV	$\emptyset_i$	Y_i	Flu. Ene in MeV	Flu. Lines
1	O	0.014699	0.242	0.0	0.0	O
2	L	0.014699	1.00	0.3032	0.012217	F_L
3.	K	0.088004	2.854	2.074	0.074969	$K_{\alpha1}$
4.	K	0.088004	3.957	3.127	0.072804	$K_{\alpha2}$
5	K	0.088004	4.570	3.712	0.084777	$K_{\beta1}$
6	K	0.088004	4.715	3.850	0.087320	$K_{\beta2}$

$$Z = 82$$

the same manner and finally, as usual, the new direction
parameters can be computed using equations given in section 2.5.

Although, the method to be followed for a Photo
electric event is described clearly in Refs. (4) and (5),
the derivation and the method of obtaining $\emptyset_i$s' and Y_is' are
not explained.

CHAPTER-3

RESULTS

In this Chapter, results, obtained by making use of the different sampling techniques that are to be followed at various stages of photon transport simulation seen in Chap.2, have been presented. All necessary data are of Israel(10) and that of mass absorption coefficient of air or tissue are from Ref. (12). In the development of a computer code for the chosen problem, three . cases have been considered to observe the improvement of results of one case over the other and ofcourse, to attain the closeness of exact physical situation also.

Observations have been made firstly, by forcing all interactions to be Compton scattering (com), secondly, by considering only two types of interactions namely Compton scattering and Pair-Production event (com+ppd), and thirdly by including all the three events viz., Compton scattering, Pair-Production and Photo electric effect (com+ppd+pee), Next section gives a brief idea about the concept of survival weights.

3.1 CONCEPT OF SURVIVAL WEIGHTS

In Monte Carlo computations, this idea of statistical weight has been included to account the absorption effect after a scattering. A particle starts from the source with a weight of unity. Obviously it has not encountered any interaction in the medium so far. The particle weight after a collision is the weight before collision multiplied by the survival ratio μ_c/μ_T (E) which is the ratio of macroscopic scattering cross section to the macroscopic total attenuation cross section.

Thus after each scattering event the weight is adjusted in the same way to account the effect of absorption of photons in the scattering. Here, one can choose R ussian Roullette method (8) to decide whether the particle survives or not.

3.2 COMPUTING DOSE

As mentioned earlier, the five mfps' shield is divided into five regions. Dose computations have been made for each mfp or region at points on the cylinder axis and along the circumference of the circle with radius equal

to that of spherical shield in the Y-Z plane to account for the dose points along the perpendicular axis of the duct. The right half circle is divided into 18 equal parts w.r. to the origin in step of 10 degrees each and hence doses computed in each interval corresponds to some amount of height in the perpendicular axis.

Though results are obtained for all the 18 intervals, assuming symmetry one can limit to only either upper half or lower half of the semicircle. From the observations, it is found that there is not significant difference in values between the two halves.

When a particle crosses a mfp, the associated particle current is converted into flux units, say T (no./cm^2- sec) and then dose rates in mR/hr can be calculated using the relation namely,

$$\text{Dose Rate} = 0.05767 \times E \times \frac{\mu_a}{\rho}(E) \times T$$

where 0.05767 is the constant which converts the unit of $E \frac{\mu_a}{\rho} T$ into dose rate mR/hr units, E is the Energy of the photon in MeV and $\frac{\mu_a}{\rho}$ is the mass absorption coefficient of air or tissue at energy E in cm^2/gm.

3.3 MONTE CARLO OUTPUT

The three cases mentioned above are given below along with the results obtained in each case.

(i) Here all interactions are forced to be Comptons scatterings i.e., absorptive events cannot occur directly. Thus the particle weight is adjusted for by a factor of survival ratio after each collision. Results obtained are shown in Figs.3.1 and 3.2. Fig. 3.1 shows the distribution of doses rates at each mfp for various angles i.e., along the perimeter of the circle.

(ii) In this, all interactions are forced to be either Compton scattering or Pair-Production event. Ofcourse if the energy of the photon is less than 1.022 MeV then all interactions are ultimately forced to be Compton scatterings. If E 1.022 MeV, then Pair-Production is considered to occur if r $\mu_C/(\mu_C + \mu_{PPD})$ where r is a random number between 0 and 1 ; otherwise it will not occur and here the survival ratio is given by

$$\text{Survival ratio} = (\mu_C + \mu_{PPD})/\mu_T$$
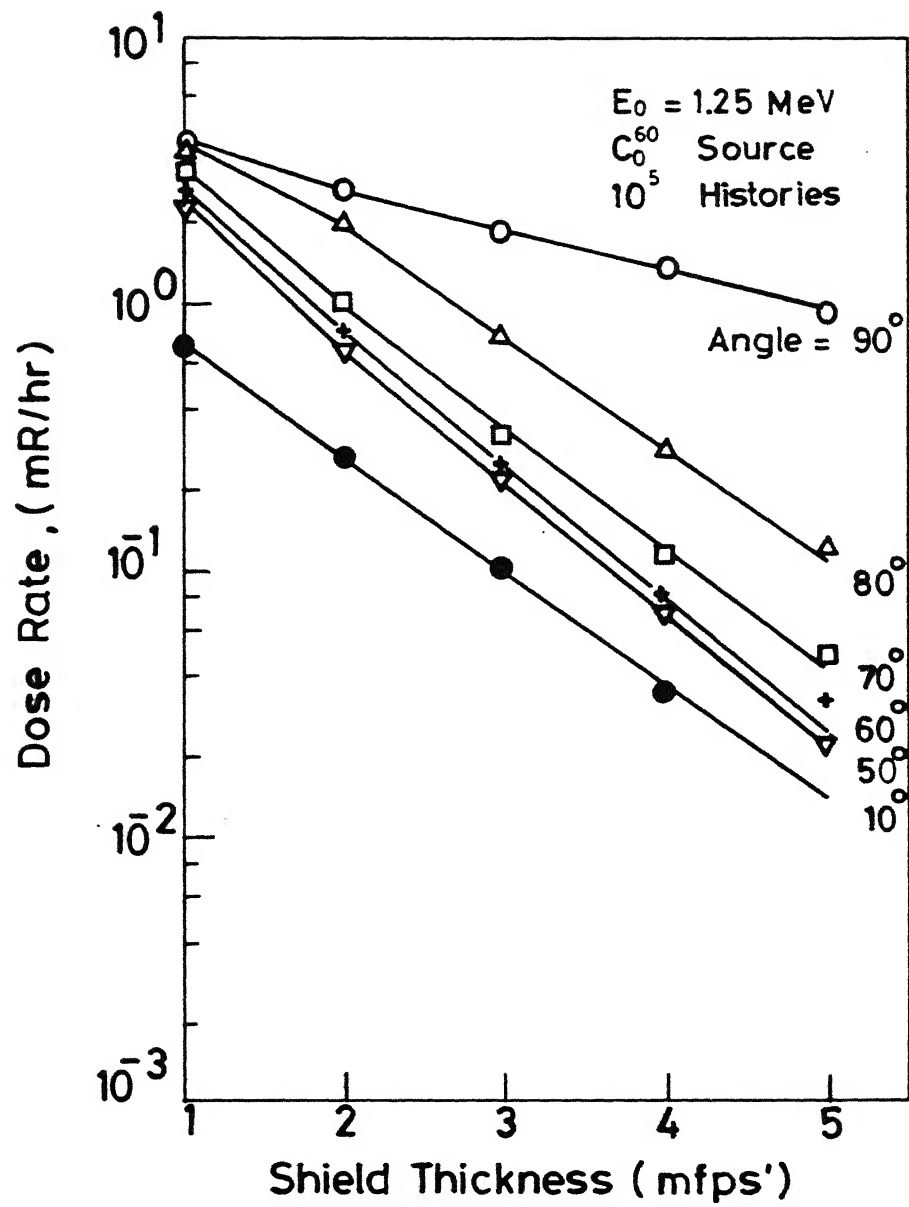
As describes in (i) above, results are shown in

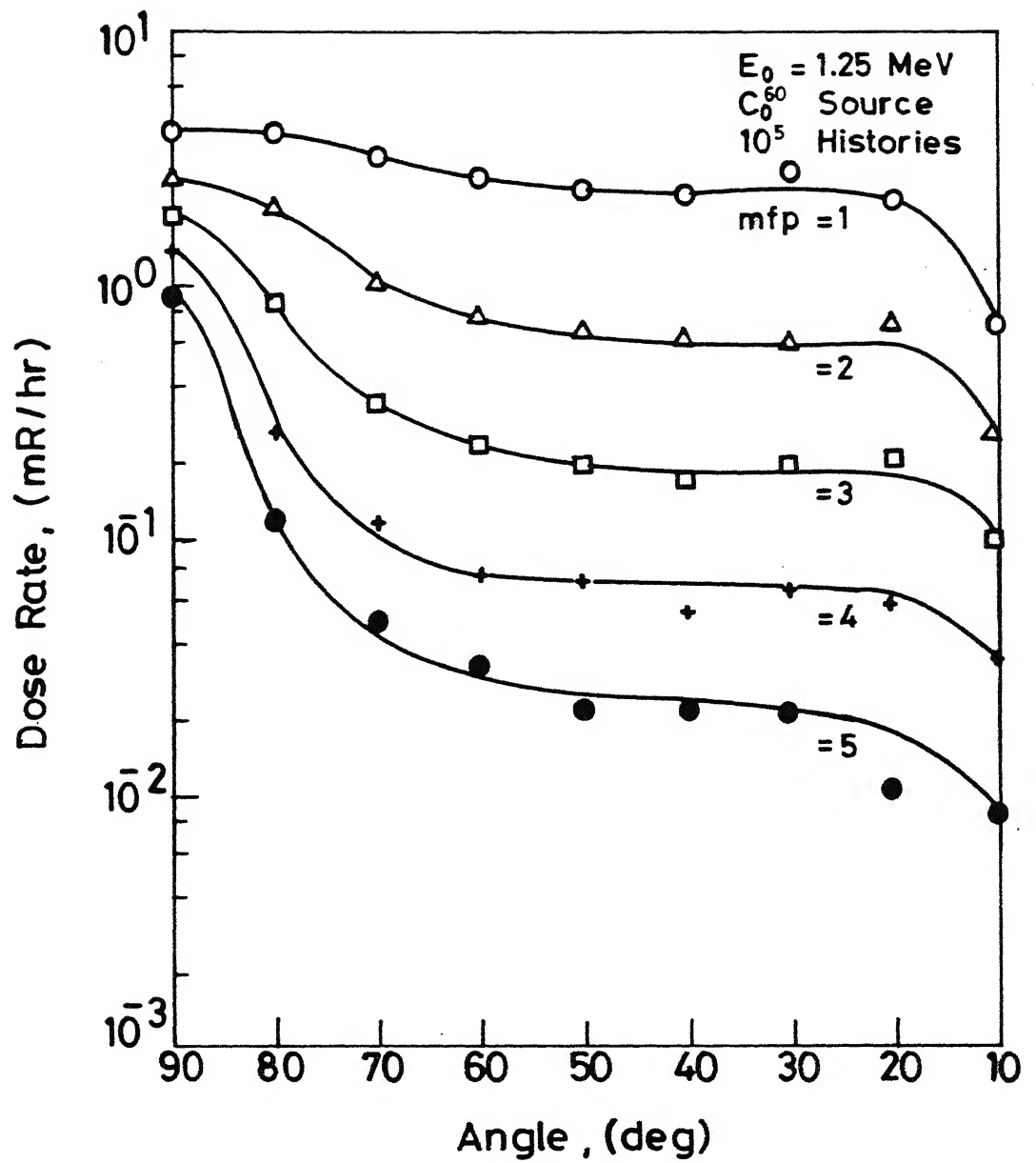Fig. 3.1   Variation of Dose with Mean Free Path (Com)

Fig.3.2 Variation of Dose with Angle (Com)

Figs. 3.3 and 3.4. Comparision study will be done later.

(iii) In this case Photo Electric effect is also included in the simulation along with other two process namely Compton scattering and Pair-Production. Now one has to decide the type of interaction to be allowed to occur at the interaction point at some energy, say E. This can be done by comparing a random number 'r' with the ratios μ_{PEE}/μ_T, μ_C/μ_T and μ_{PPD}/μ_T. i.e., if r lies between μ_{PEE}/μ_T and μ_C/μ_T. (Say $\mu_{PPD} < \mu_{PEE} < \mu_C$ at E), then the Compton scattering will occur. Likewise the choice of the event may be decided at any energy E.

Here also the particle weight after an event is modified by the factor survival ratio $(\mu_{PPD} + \mu_C)/\mu_T$. In the case of Photo electric effect, if fluorescent emission is allowed then the particle will survive with that fluorescent energy otherwise its life will be terminated. Results obtained in the case are shown in Figs.3.5 and 3.6.

3.4 COMPARISION OF MONTE CARLO OUTPUT WITH ANALYTICAL METHODS

A semi-analytical approach for radiation streaming through a cylinderical duct has been made satisfactorily by Tsuro et.al. (11). First this method was applied to the case
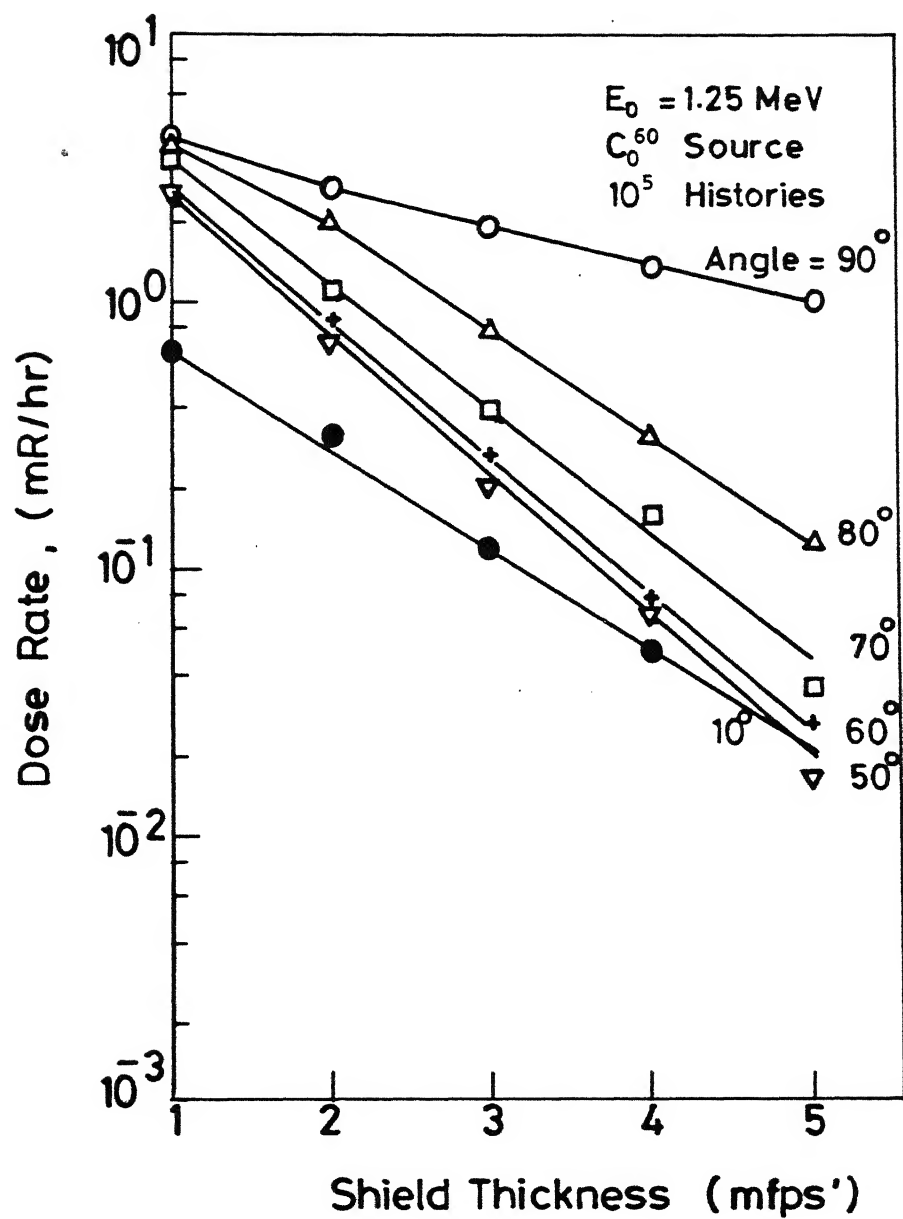
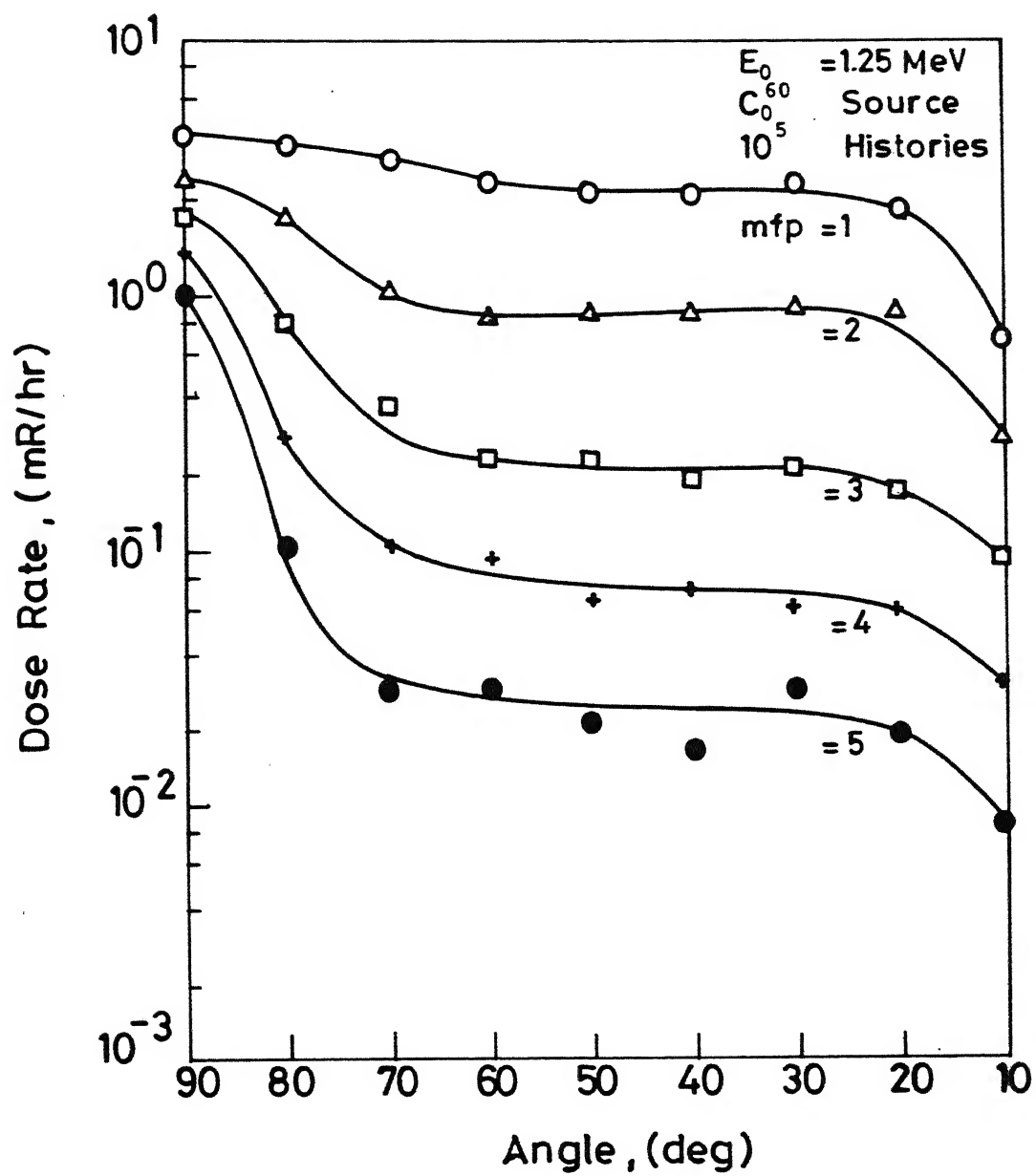Fig. 3.3   Variation of Dose with Mean Free Path (Com+PPD)

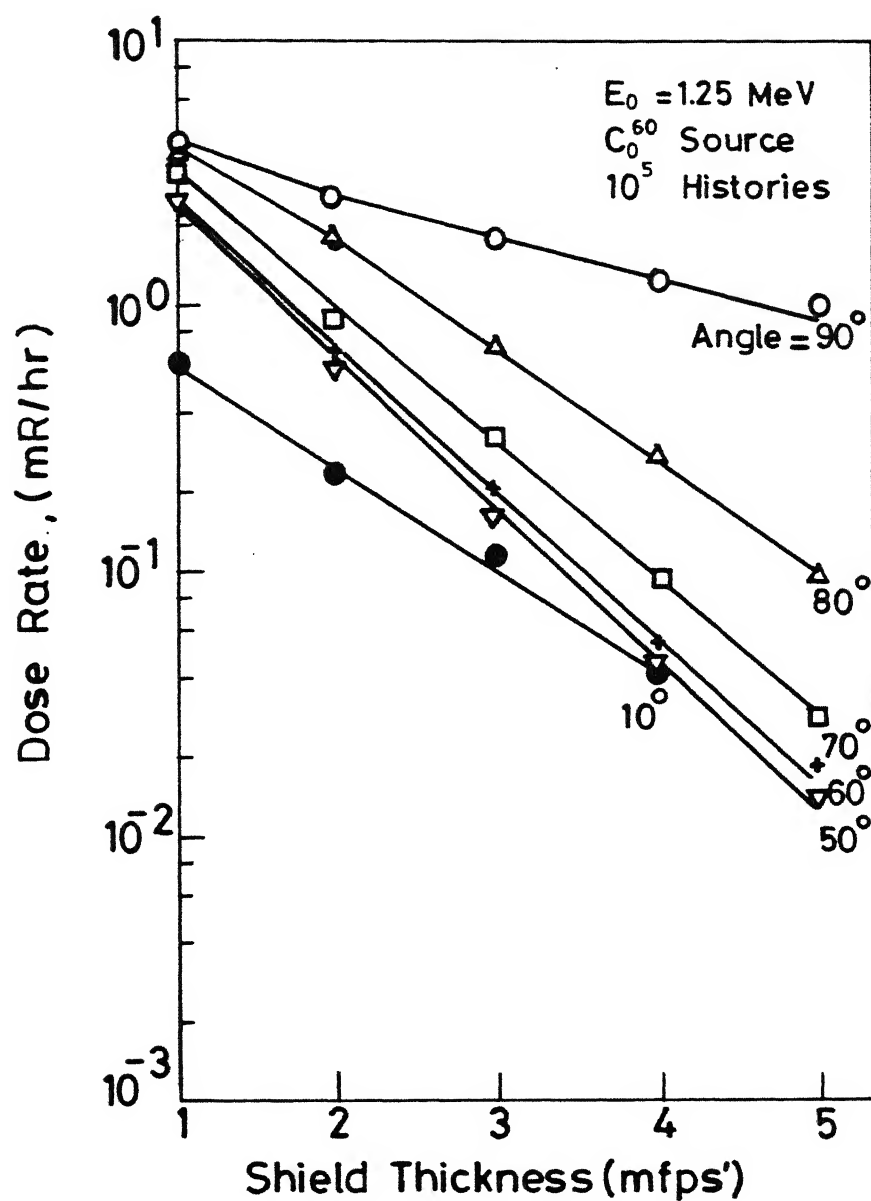Fig. 3.4 Variation of Dose with Angle (Com+PPD)

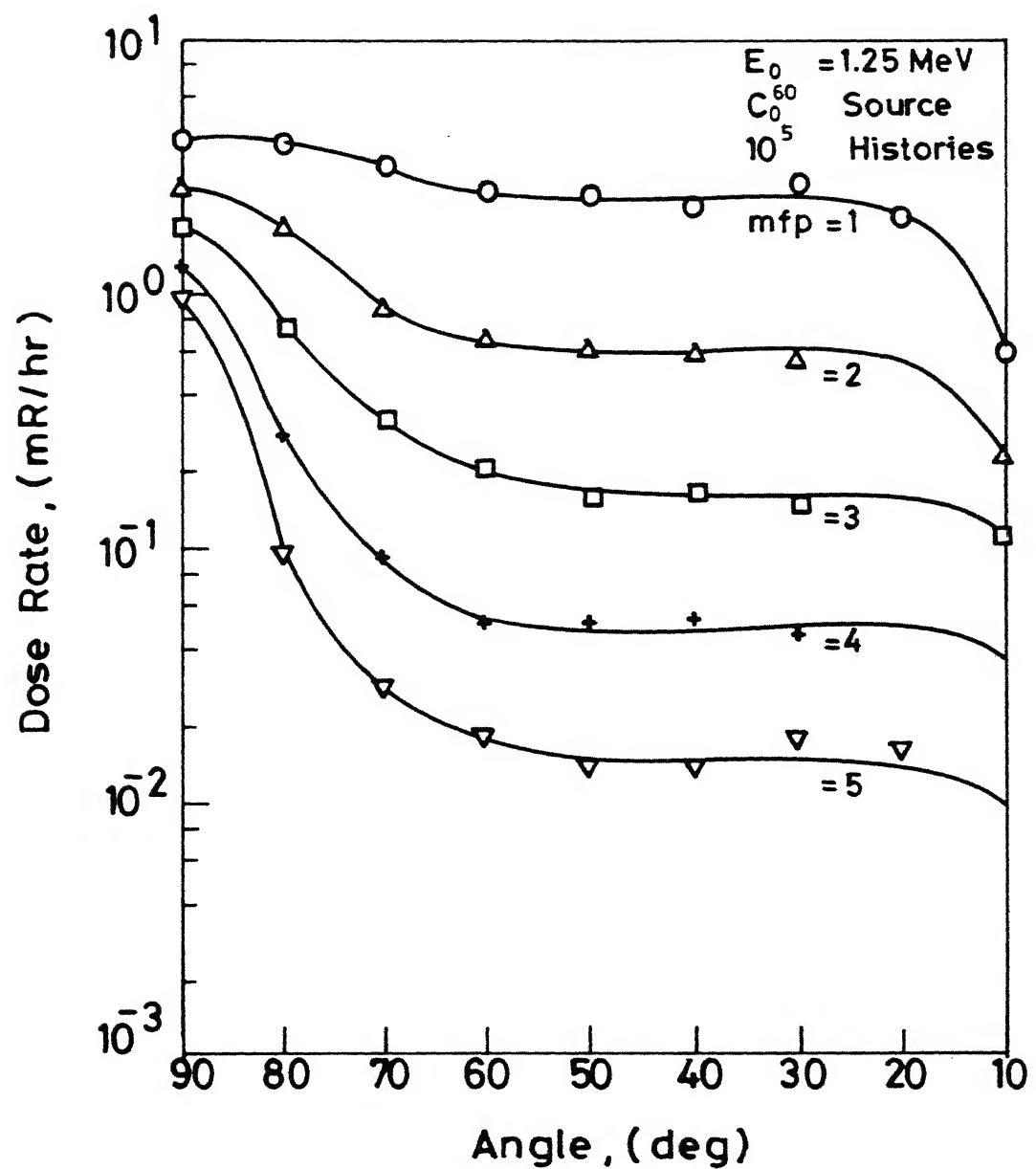Fig. 3.5 Variation of Dose with Mean Free Path (Com + PPD + PEE)

Fig.3.6 Variation of Dose with Angle (Com+PPD+PEE)

of Gamma ray streaming after single scattering in a duct for a disc source at its entrance. Later, it was modified to include multiple scatterings also. The dose due to single scatterings or singly scattered dose at the duct exit in given by

$$D_{SCA} = \pi R_0^2 \int_0^L dz \int_0^{+\infty} \frac{r\, f}{\mu_0} \quad \frac{d\Sigma}{d\Omega} \quad \frac{1}{D_0^2\, D_1^2}$$

$$\exp(-\mu_0 d_0 + \mu_1 d_1) \quad E_1 \quad \frac{\mu_{air}}{\rho}(E_1) \quad df \quad \ldots.(3.1)$$

where   L and R_0 are the length and radius of the duct respectively

μ_0 : initial attenuation coeficient of photon

μ_1 : attenuation coefficient of photon after scattering

d_0 : sampled path length

d_1 : distance between scattering point and detector minus the path across the duct

D_0 : distance between the point of origin and the scattering point

D_1 : distance between the scattering point and the detector

f : an integral parameter and $r = R_0 + f^2/\mu_0$

E_1 : the photon energy after scattering

and $\mu_{air}/\rho (E_1)$ is the energy absorption coefficient of air at energy E_1.

The total dose at any point on the duct axis is the sum of unscattered dose and scattered dose, and the unscattered dose at any point 'L' units away from the disc source is given by (9)

$$D_{uns} = \frac{S_A}{4} \; E_0 \; \frac{\mu_{air}}{\rho}(E_0) \; \ln (1 + R_0^2/L^2) \qquad \ldots\ldots(3.2)$$
$$X \; 0.0567$$

where S_A is the flux and E_0 is the initial energy of photon (at source).

Estimation of dose rates by analogue method is as follows. Attempts were made first, to calculate the doses along the duct axis and later for points off the axis. As such, no point detector calculation, say a particular point in the shield, can be done straight away using this method but the normal procedure is to consider some distance $\pm \Delta d$ about that point along the boundary so that the sum of the individual contributions of each particle's dose within that total $2 \Delta d$ length will be considered, effectively, as the dose about that point. Ofcourse, the same procedure has to

be followed for all points of interest. Finally one can get a histogram, say dose vs shield thickness, and from that, distribution of doses along the points of interest may easily be found.

Now, the question arise, is, how to choose the interval Δd for a given problem?. As such, there is no specific rules or procedures regarding this. Perhaps some experienced workers might guess the procedure to be followed for a problem of interest by intution. But in this work, few approaches have been made and the results obtained are shown in Figs.3.1 to 3.6.

In the first approach 0.5 and 1.0 were considered for Δd_z values i.e. Δd along Z axis (refer Fig. 2.1) in two trials. It was found unsatisfactory for even points on the duct axis because the values of total dose computed minus the unscattered dose computed from equation 3.2 were much higher than the unscattered doses (values are not shown here).

Further some results were obtained for points off the axis also using the same approach. Here, the same $2\Delta d$ length cannot be considered for every $2\Delta d$, the arc length

(boundary) is not constant. So it is better to consider equal angles, i.e. divide each mfp into eighteen 10 degree intervals, instead of equal heights. Though this helped to remove the difficulty faced due to the unequal arc lengths, again, the magnitudes of doses were high.

In the next approach, in addition to Δd_z value, Δd_x i.e. along X axis also included to observe the effect on dose values. $\Delta d_z = 0.5$ and $\Delta d_x = 0.5$, showed erratic results. Later when Δd_x increased from 0.5 to 1.0 (equal to the radius of the duct), satisfactory results have been obtained as shown in Table 3.1 for dose points on the duct axis.

Assuming that the above fixed values of Δd_x and Δd_z are valid for points off the axis also, observation have been made for various angles and the results are shown in Figs. 3.1, 3.3 and 3.5. For e.g., Fig. 3.1 shows the distribution of dose rates for various shield thicknesses at each angular intervals, while Figs. 3.2, 3.4 and 3.6 show the distribution of dose rates for various points on the surface of the shield in each mfps'.

The computed multiple scattered doses on the axis are shown in Table 3.1 for the three different cases, mentioned

Table 3.1 Comparison of Monte Carlo Dose Rates with
Singly Scattered Dose Rates

MFP	Distance in cm	Dose* mR/hr	Dose M.C. case (i)	Dose ** Error iin %	Dose M.C. case(ii)	Error in %	Dose M.C. case(iii)	Error in %
1	2.547	—	9.3920	—	9.6450	—	9.417	—
2	4.0931	2.8559	3.7700	-37.0	3.974	-39.0	3.701	-30.0
3	5.6396	1.8034	2.050	-14.0	2.191	-21.0	1.986	-10.0
4	7.1861	1.1070	1.351	-22.0	1.347	-22.0	1.233	-11.0
5	8.7327	0.7477	0.8921	-19.0	0.9033	-20.0	0.875	-17.0

* = Single Scattered Dose

** = Error = $\dfrac{\text{Single Scattered Dose} - \text{Monte Carlo Dose}}{\text{Single Scattered Dose}}$ (M.C.)

Distance = Duct Radius + No. of mfps'/μ_o $(R_o =$

in section 3.3, considered for obtaining these results. These values are compared with the singly scattered doses computed using equation(3.1).

For water at 1.00 MeV photons (survival ratio 1.0 and for $L/R_0 = 10$; the ratio of maximum shield thickness to duct radius), it i s seen that (9) the ratio between scattered and unscattered dose is about 40%. So,for lead, at 1.25 MeV (survival ratio approximately 0.8) and for L/R_0 9.0, it is expected that approximately the same 40% will be the scattered dose. Table 3.2 shows not much difference between the Monte Carlo output and the assumed values.

As is known that monoenergetic photons incident upon a shield emerges from the shield with a continuous energy say from 0 to E_0 (the maximum energy E_0). So emphasis has been shown to count the number of particles falling in an energy interval, say in step of 0.1 MeV from 0.0 to 1.25 Mev, while crossing a region or boundary of interest. Further this observation will put light on the difference between one case and the other (see section 3.3). The observed number of particles for different energies at each mfp are shown in Figs. 3.7 and 3.8.

3.5 DISCUSSIONS

In the Figs. 3.1, 3.3 and 3.5 curves are not drawn for angles 20°, 30° and 40° because the computed values for these angles lie close to each other. The computed value of dose at the fifth mfp at angle 10° is 0.0 in all the three cases considered and this point is not shown in all the three figures mentioned above. In practice, there is some contribution from a disc source to that point and hence this gives rise to doubts about the choice of the $\triangle d_Z$ and $\triangle d_X$ values chosen. A suggested approach is given in Chap. 4.

Further, number of particles escaping through the duct (i.e. part of the uncollided flux) is found to be approximately 620 in all the three cases considered for 10^5 source particles. Since the source energy is only 1.25 MeV there is not much difference between curves in Figs. 3.1 and 3.3, and, Figs. 3.2 and 3.4 because Photo electric effect which accounts for absorption is not included. But the same figures compared with Figs. 3.5 and 3.6 which include Photo electric effect show some difference in the dose values.

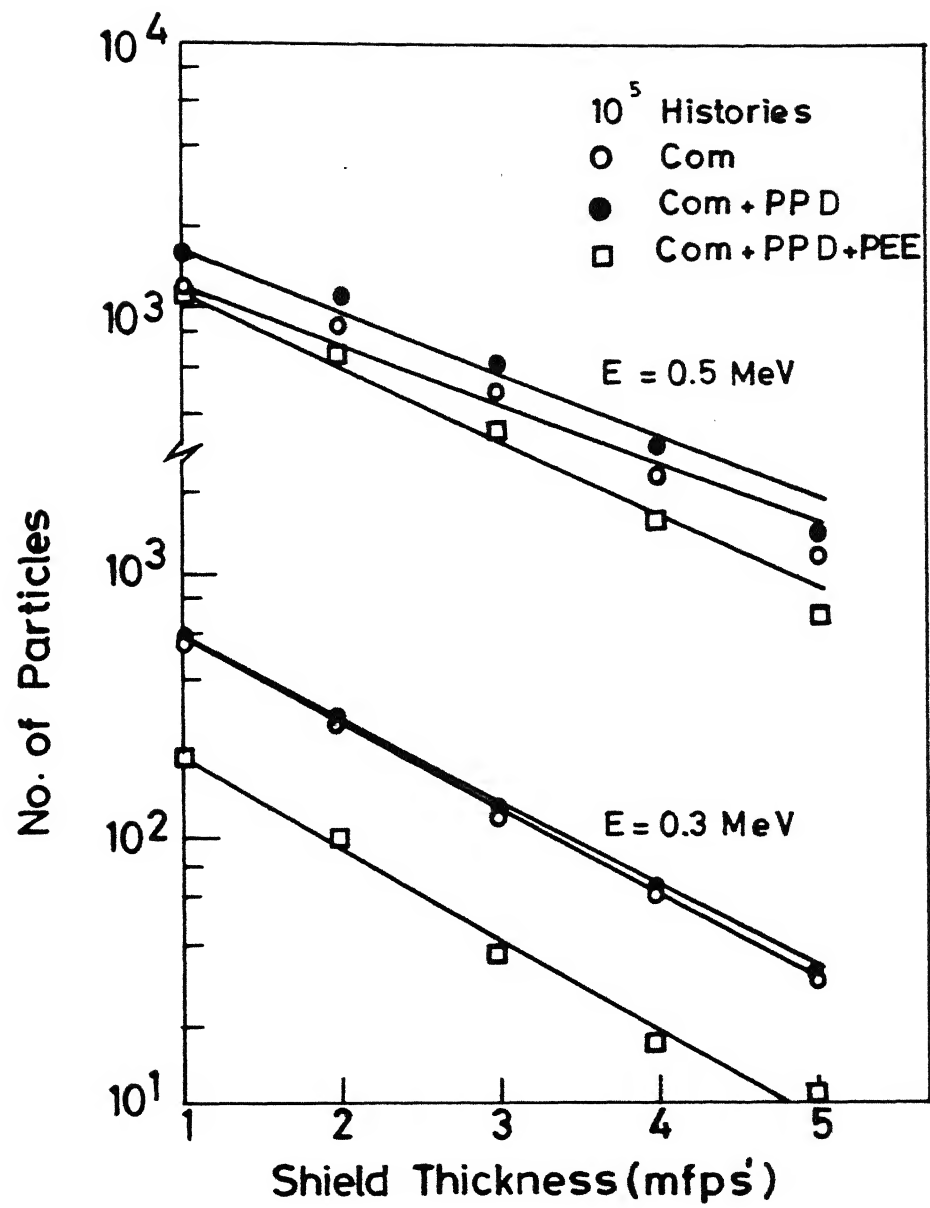As mentioned earlier, the number of particles having

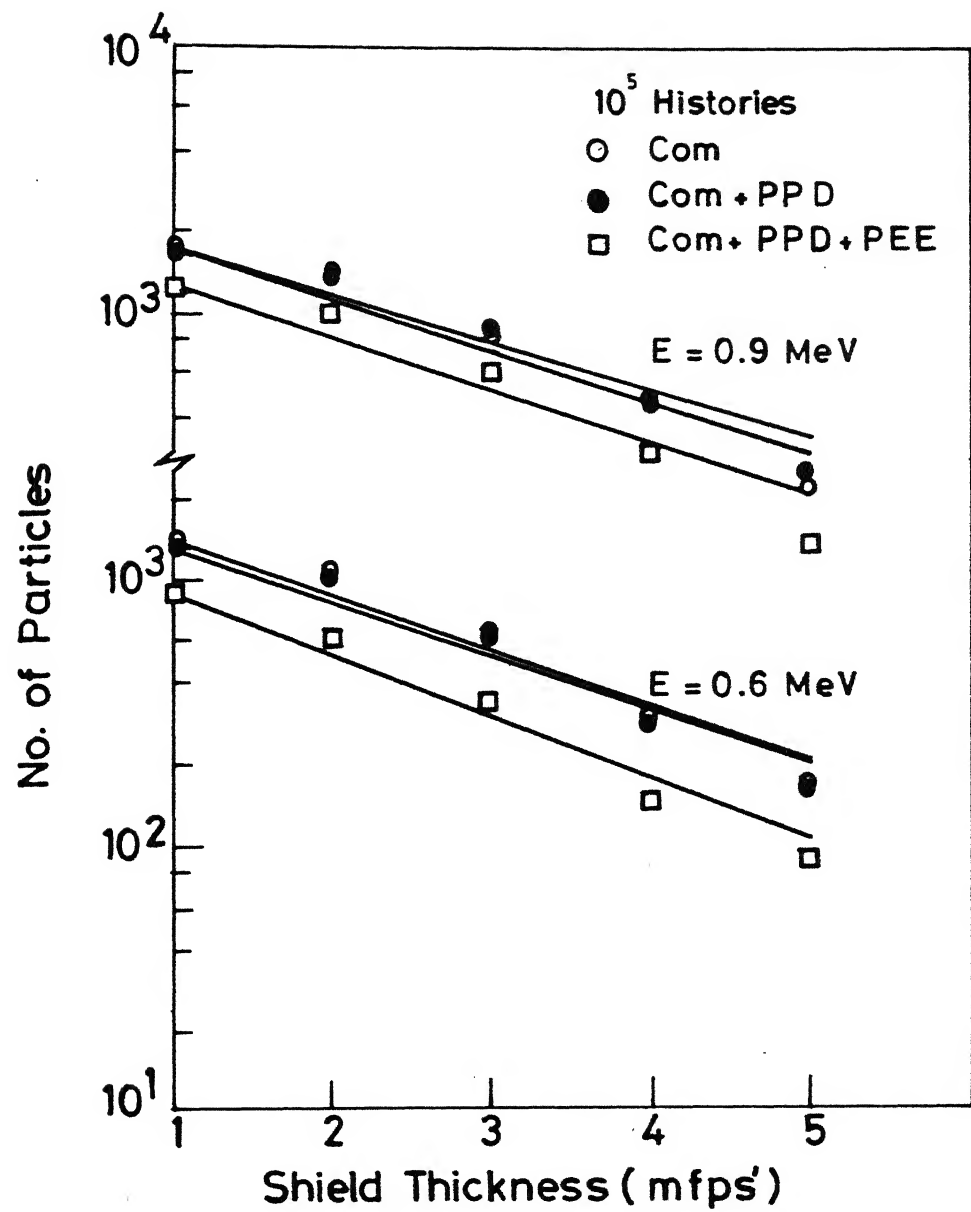Fig. 3.7   Variation of No. of Particles with Mean Free Path.

Fig. 3.8 Variation of No. of Particles with Mean Free Path.

Table 3.2 Comparision of Monte Carlo Dose Rates
with modified Dose Rates (40% above unscattered)

MFP	Distance in cm	Dose* mR/hr	Dose M.C. case (i) mR/hr	Dose M.C. case (ii) mR/hr	Dose M.C. case(iii) mR/hr
1	2.547	—	9.392	9.6450	9.417
2	4.0931	3.9203	3.770	3.9740	3.701
3	5.6396	2.0933	2.050	2.1910	1.986
4	7.1861	1.2967	1.351	1.3470	1.233
5	8.7327	0.8809	0.892	0.9033	0.875'

* Unscattered Dose + 40% Unscattered Dose

particular energy as a function of distance in mfps' are
shown in Figs. 3.7 and 3.8. Four sets of curves for energies
0.3, 0.5, 0.6 and 0.9 MeV are shown in those figures. Here
again, due to absorption in all the four sets, the inclusion
of Photo electric effect shows lower values. The amount
decreased from that of the other two cases is about 30% to
65%. At 0.5 MeV, the contribution due to Pair-Production is
more compared to other energies because of the annihilation
gammas

CHAPTER-4

CONCLUSIONS AND RECOMMENDATIONS

4.1 CONCLUSIONS

The following conclusions can be drawn based upon the results of the present study.

1.   Results have been obtained by using Monte Carlo methods for the investigation of photon transport in a chosen shield geometry shown in Fig. 2.1. Computed Gamma ray dose rates along the axis of the duct are shown in Table 3.1. Those values have good agreement with the results obtained by Tsuro et. al (11).

2.   No comparision has been made for the doses computed at points off the duct axis because neither analytical solutions nor experimental results are available.

3.   In the simulation of photon transport, all the three events Photo electric effect, Pair-Production and Compton scattering are included and the effects of

absorption due to Photo electric effect and Pair-Production are found clearly from Figs. 3.7 and 3.8.

4. From the values obtained for points in the source plane, (refer section 3.5), one can conclude that the values of $\triangle d_Z$ and $\triangle d_X$ are not reliable.

4.2 RECOMMENDATIONS

1. For the dose calculations, the values of $\triangle d_Z$ and $\triangle d_X$ may be changed or the whole scheme of particles scoring should be modified suitably to calculate the flux accurately. This can be done, for e.g., as follows. Divide the perimeter of the semi circle into 18 intervals, try to make a circle about each such interval so that the area under each circle remains constant and hence, the number of particles crossing each circle can be calculated.

2. This investigation can be carried out by including some biasing techniques for path length selection and depending upon the interest, directional biasing may also be included.

3.   Simulation approach can be extended to shields made of heterogeneous materials or to multilayered shields.

BIBLIOGRAPHY

1. Blomquist, R.N. and Gelbard, E.M. (1983). An Assessment of Existing Klein-Nishina Monte Carlo Sampling Methods. Nucl. Sci. Engg., 83, P. 380

2. Carter, L.L. and Cashwell, E.D. (1975). Particle Transport Simulation with the Monte Carlo Method. USAEC Report TID - 26607

3. Cashwell, E.D. and Everett, C.J. (1959). A Practical Manual on the Monte Carlo Method for Random Work Problems. Pergamon, Oxford

4. Cashwell, E.D. et al. (1973). Monte Carlo Photon Codes: MCG and MCP. USAEC Report LA - 5157 - MS Los Almos Scientific Laboratory

5. Everett, C.J. and Cashwell, E.D. (1973). MCP Code Fluorescence - Routine Revision. USAEC Report LA - 5240 - MS Los Almos Scientific Laboratory

6. Khan, H. (1950). Random Sampling (Monte Carlo) Techniques in Neutron Attenuation Problems - I. Nucleonics., Vol. 6, No. 5, P. 27

7. Khan, H. (1954). Applications of Monte Carlo. USAEC Report AECU - 3259, Rand Corporation (cited in Ref. 12)

8. Schaeffer, N.M. (Ed.).(1973). Reactor Shielding for Nuclear Engineers. USAEC Report TID - 25951

NETP-1986-M-PAN-GAM